Shape and internal structure of silver nanoparticles embedded in glass

H. Hofmeister[a] and G.L. Tan[b]
Max Planck Institute of Microstructure Physics, D-06120 Halle, Germany
M. Dubiel
Department of Physics, University of Halle-Wittenberg, D-06108 Halle, Germany

(Received 19 November 2004; accepted 21 March 2005)

The structural characteristics of silver nanoparticles embedded in glass by various routes of fabrication were studied in detail using high-resolution electron microscopy to find out if they are influenced by interaction with the surrounding glass matrix. Besides the formation conditions, the strength of the interaction between metal and glass governs the size-dependent changes of lattice spacings in such nanoparticles. However, determination of these changes is not straightforward because of complicated particle configurations and the interference nature of the lattice imaging technique. Imaging of lattice plane fringes and careful diffractogram analysis allowed the exclusion of any kind of tetragonal lattice distortion or transformation to hexagonal lattice type that may be deduced at first sight. Instead, the formation of twin faults in these nanoparticles turned out to be the essential structural feature and the main source of confusion about the lattice structure observed. The variety of particle forms is comparable to particles supported on oxide carriers. It is composed of single-crystalline particles of nearly cuboctahedron shape, particles containing single twin faults, multiple twinned particles containing parallel twin lamellae, and multiple twinned particles composed of cyclic twinned segments arranged around axes of 5-fold symmetry. The more twin planes involved in the particle composition, the more complicated is the interpretation of lattice spacings and lattice fringe patterns due to superposition of several twin segments.

I. INTRODUCTION

The structural characteristics of metal nanoparticles become more important the more they are used in structure-sensitive processes such as heterogeneous catalysis[1] or applications such as selective optical absorbance.[2] For the latter purpose, incorporation of the nanoparticles in a transparent and durable host is required. Nearly spherical metal particles of nanometer dimensions embedded in soda-lime silicate glass can be fabricated by several means. Their optical properties, promising for potential applications, depend on concentration, size, shape, spatial arrangement and configuration of the nanoparticles.[3,4] Conventional experimental routes of synthesis like Na^+/Ag^+ ion exchange plus thermal processing enable only minor variations of these structural characteristics.[5] Large volume fractions of nanoparticles arranged in a near-surface region of glassy hosts may be obtained by high-energy ion implantation plus thermal processing.[6] The formation of metal nanoparticles in glass may be accompanied by the generation of tensile or compressive stresses due to thermal expansion mismatch[7] and/or radiation damage in the glass matrix.[8] The lattice spacings of crystalline nanoparticles sensitively reflect their state of stress depending on the respective formation conditions.[9]

There is one cause of stress due solely to their small dimensions. Because of their large surface-to-volume ratio A/V, nanoparticles with free surface may exhibit a considerable lattice contraction Δa due to the hydrostatic pressure Δp caused by the surface stress f. For isotropic solids, f consists of the specific free surface energy σ and the contribution of elastic deformation to a reversible surface change $f = \sigma + A \cdot d\sigma/dA$. For spherical particles of radius r the capillary pressure Δp is given by $\Delta p = 2f/r$, from which with the compressibility $K = -\Delta V/V \cdot \Delta p$ the lattice contraction $\Delta a = -2aKf/3r$ is obtained as function

[a]Address all correspondence to this author.
e-mail: hof@mpi-halle.mpg.de
[b]Present address: Materials Science Department, University of Pennsylvania, 3231 Walnut Street, Philadelphia, PA 19104.
DOI: 10.1557/JMR.2005.0197

of the radius of curvature r. Thus, f may be calculated from the size-dependent lattice contraction determined by means of high-resolution electron microscopy (HREM).[9,10] For anisotropic solids, f is the mean value of the various crystal facets forming the surface of the nanoparticle. For nanoparticles embedded in a matrix of foreign material the surface stress f must be replaced by the interface stress f^* representing the elastic response of the interface between both materials to elastic deformation. It is related to the strength of interaction, i.e., the adhesion work, of the phases adjacent to the interface.

For particles of transition metals like Pd, Ag, or Au with sizes well below 10 nm, most routes of synthesis produce a great variety of particle shapes accompanied by variations of the internal structure.[11] This multitude of configurations may be understood in terms of the great ease of structural transformations during particles growth.[12] Besides single crystalline particles that may exhibit the shapes of truncated octahedra or cuboctahedra, single twinned particles of both shapes are found. The formation of twin faults where the twin plane forms a boundary between the twinned subunits situated in mirror symmetry to each other is a characteristic of face-centered-cubic (fcc) metal nanoparticles.[13] Such twins may form via nucleation or as a result of erroneously attaching atoms or molecules to a crystal during growth. Repeated twinning on parallel planes results in parallel twin lamellae, while multiple twinning on alternate coplanar planes produces cyclic twins with the twinned segments arranged around 5-fold axes.[14–16]

Since the latter kind of arrangement does not fit into the characteristics of the fcc crystal lattice but suffers from a lack in space filling, there is some lattice distortion required for the cyclic twinned polyhedra, i.e., decahedron and icosahedron. Homogeneous distortions corresponding to transformation of the fcc lattice of all twin segments to body-centered orthorhombic or rhombohedral lattice are discussed[17] as well as inhomogeneous distortions where the lattice in only one or a few segments is thought to undergo distortion to base-centered tetragonal lattice.[18] Alternatively, at small enough sizes, the angle deficit may be shared around all twin boundaries by incorporation of additional lattice defects like stacking faults. Furthermore, there are reports in the literature about the observation of hexagonal close-packed (hcp) structure in fcc metals at small dimensions.[19] However, by careful analysis, this interpretation can be mostly ruled out in favor of a particular orientation of single twinned nanoparticles.[20]

It is the aim of this work to give an overview of the variety of forms of silver nanoparticles incorporated in glass by various routes of fabrication and discuss their structural characteristics as studied by high resolution electron microscopy. Since the issue of the stress state of these nanoparticles depending on the fabrication conditions is treated elsewhere,[21,22] here we present characteristic structural features of the most frequently occurring particle forms by combining HREM imaging of lattice plane fringes, diffractogram analysis, and model considerations, taking into account image contrast calculations. This may help to interpret the image contrast of particles of various content of twin faults in terms of tilting with respect to the electron beam and double diffraction due to superimposed twin segments.

II. EXPERIMENTAL

The silver nanoparticles were prepared either by thermochemical processing (i.e., Ag^+/Na^+ ion exchange) or high-energy ion irradiation (i.e., Ag^+ ion implantation) of commercial soda-lime silicate float glass. For the ion-exchange route, glasses containing 72.4% SiO_2, 13.8% Na_2O, and 6.4% CaO as main constituents were used the glass transformation temperature T_g of which is ~535 °C. The ion exchange procedure involved immersing the glass in a mixture of molten $AgNO_3$ (2 wt%) and $NaNO_3$ (98 wt%) held at 330 °C. Due to the presence of some Fe^{2+} as thermo-sensitive reducing agent, silver ions diffused into the glass were reduced to Ag^0 and precipitated so as to form embedded silver nanoparticles. Subsequent annealing at elevated temperatures (480–650 °C) was applied to increase size and penetration depth of the silver nanoparticles.[21] To allow for different thermal stress built-up within the glass, different cooling procedures to room temperature were applied: slow cooling inside the furnace, cooling in ambient air, and rapid quenching on a metal plate.[9]

For the ion implantation route commercial soda lime glasses of nearly the same composition as above but with distinctly lower iron content, were used. Both types of glass were selected for this study because of their notably low tendency to undergo phase separation and crystallization upon electron beam irradiation. Ag^+ ions of 200 keV energy were implanted at room temperature to doses of 0.5×10^{16} to 2×10^{16} Ag^+ ions/cm^2 using a beam current density in the range of 0.5–2 mA/cm^2.[8] To avoid charge buildup during implantation, the glass surface was simultaneously exposed to electron beam irradiation. At high enough fluence silver nanoparticles are formed in a thin region of the glass very near to the irradiated surface. Subsequent annealing at elevated temperatures can be applied to increase the size and modify the depth distribution of the particles.[22]

For electron microscopy examination, the glasses containing silver nanoparticles were cut into thin slices, mechanically ground and polished, and finally processed by argon ion beam thinning. A thin carbon film was deposited on both sides of the specimens to avoid charging by the electron beam.[9] For HREM work, a JEM 4010 (JEOL, Tokyo, Japan) operating at 400 kV was used and recording of micrographs of silver nanoparticles was

done at optimum defocus settings (near Scherzer focus).[7] Real space and reciprocal (Fourier) space image processing making use of the Digital Micrograph and the NIH Image[23] software were applied to selections of digitized micrographs for contrast enhancement and image evaluation by diffractogram analysis at individual silver nanoparticles. Image contrast calculations for silver nanoparticles of truncated octahedron shape were carried out using the Mac Tempas multislice algorithm.[7]

III. RESULTS AND DISCUSSION

A. Variation of particle forms

The appearance of silver nanoparticles embedded in glass may vary in wide ranges depending on the respective route of fabrication applied. Here we do not consider the number density of particles within a certain glass volume, their size distribution, and any specific way of particle arrangement, but will focus on particle shape and internal structure. In general, we can state that the variety of particle forms does not differ from that of particles supported on oxide carriers or of other origin.[24] It is composed of single crystalline particles of nearly cuboctahedron shape, particles containing single twin faults, multiple twinned particles containing parallel twin lamellae, and multiple twinned particles composed of cyclic twinned segments arranged around axes of 5-fold symmetry, which will be treated in detail below. There is also no principal difference concerning the fabrication of embedded silver nanoparticles in glass by ion exchange and ion implantation, regardless of subsequent thermal processing and different cooling procedures applied.

However, there is a certain preference of some forms found to be different, probably because of different growth conditions. Therefore, it has been observed that silver nanoparticles formed in soda-lime-silicate glasses of rather low iron oxide content less frequently exhibit twin faults of any configuration. On the other hand, ion implantation, mostly applied to glasses poor in iron oxide, causes distinctly more parallel lamellar multiple twins than found in glasses doped by ion exchange. Multiply cyclic twinned particles of decahedron shape (see schematic representation in Fig. 11) obviously occur at all fabrication conditions of silver particles in glass with nearly the same frequency. Multiply cyclic twinned particles of icosahedron shape (schematic representation in Fig. 15) are extremely scarce in ion implanted glasses while they have been observed a little bit more frequently in ion exchanged glasses subjected to rapid cooling from the temperature of thermal processing than in others.

B. Single-crystalline and single-twinned nanoparticles

HREM imaging of single-crystalline silver nanoparticles embedded in glass mostly displays lattice plane fringes according to the respective zone axis orientation superimposed to a certain extent of darkening due to diffraction and mass absorption of silver metal in contrast to the uniform appearance of the surrounding glass matrix. Mainly, there are to be recognized low index fringes of {111} and {200} type corresponding to particles in ⟨110⟩ zone axis orientation or of {200} and {220} type corresponding to particles in ⟨001⟩ zone axis orientation, provided there is only minor deviation from the exact orientation. Figure 1 shows an example of the

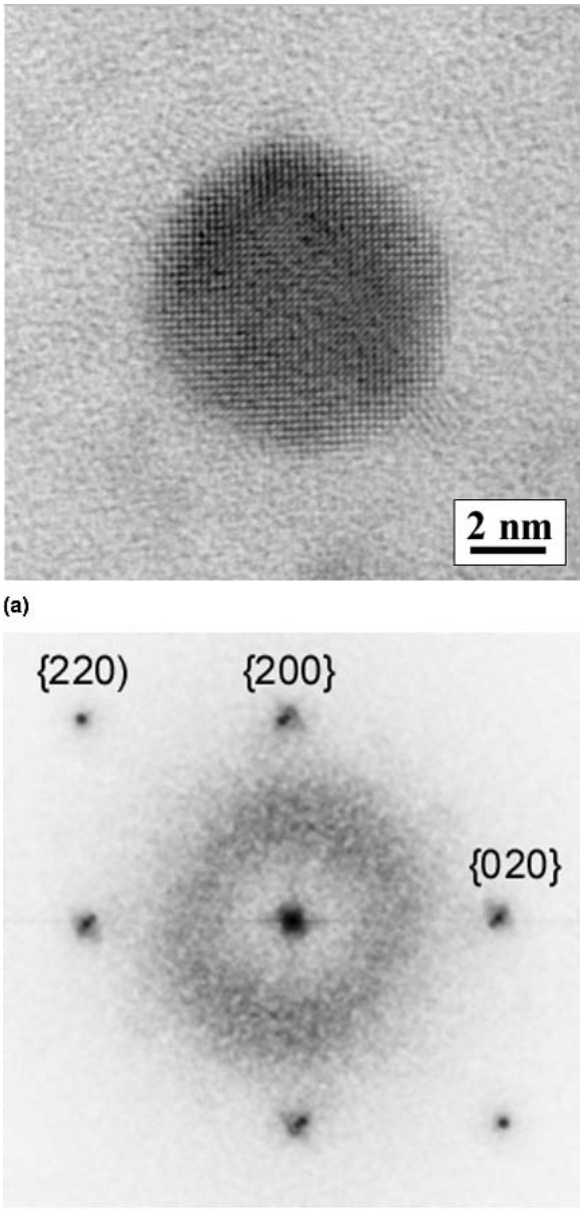

FIG. 1. (a) HREM image of a silver nanoparticle in ⟨001⟩ zone axis orientation and (b) corresponding diffractogram with indication of the reflections resulting from lattice plane fringes. The nearly circular appearance of the particle image is due to a cuboctahedron shape [see Fig. 6(a)] with some rounding of ⟨110⟩ edges.

latter orientation and the corresponding diffractogram with indication of the involved reflections. The nearly circular appearance of the particle image is due to a cuboctahedron shape with some rounding of ⟨110⟩ edges. A cuboctahedron is schematically drawn in Fig. 7(a). For a ⟨001⟩ zone axis orientation, the electron beam is directed perpendicular to one of the squared faces. Figure 2 shows an example of a single-crystalline particle in ⟨110⟩ zone axis orientation together with the diffractogram that exhibits reflections due to two sets of {111} lattice plane fringes and one of {200} planes. By comparing the image in Fig. 2(a) to the model in Fig. 7(a) the four bounding faces of {111} type and the two of {100} type, being parallel to the electron beam, may be recognized.

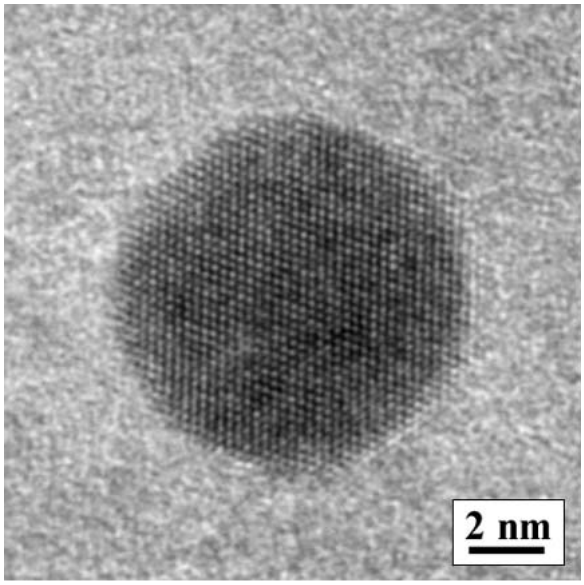

(a)

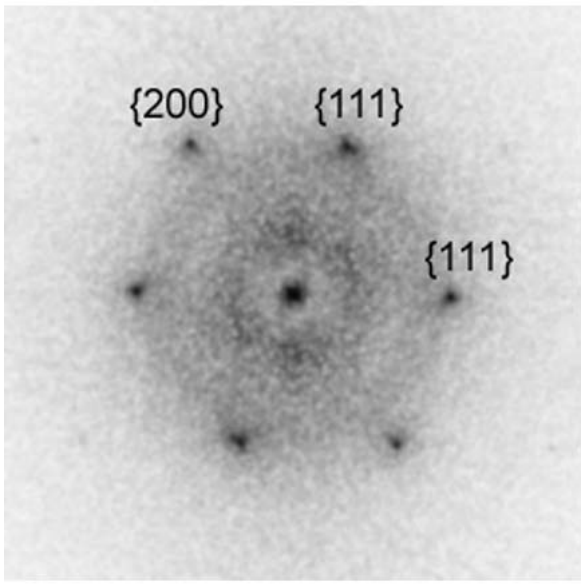

(b)

FIG. 2. (a) HREM image of a silver nanoparticle in ⟨110⟩ zone axis orientation and (b) corresponding diffractogram with indication of the reflections resulting from lattice plane fringes. The area of the particle image is bounded by ⟨111⟩, ⟨100⟩, and ⟨110⟩ edges pointing to a nearly cuboctahedron shape comparable to that of Fig. 1.

HREM imaging of lattice plane fringes is very sensitive to deviation from the zone axis orientation. A slight tilting away from this direction leads to distinct worsening of the image contrast in addition to the deterioration caused by the glass matrix surrounding the particles and the carbon coating on both sides of the specimen, which considerably limit the effective resolution. Therefore, only a minor fraction of single-crystalline silver nanoparticles in glass may exhibit lattice plane fringes. To illustrate the effect of misorientation, Fig. 3 shows two steps of an image contrast calculation tilting series for a silver nanoparticle of about 3000 atoms configured according to the fcc lattice of bulk silver. In the model of truncated octahedron shape with distinct rounding of ⟨110⟩ edges, two faces of {100} type are marked as well as the ⟨110⟩ direction of the electron beam applied for the calculation [Fig. 3(a)]. Shown here are the results obtained for typical microscope parameters (400 kV accelerating voltage, 1.0 mm spherical aberration coefficient, 8 nm defocus spread, 0.6 mrad beam divergence) and −35 nm defocus setting for an untilted particle [Fig. 3(b)] and one that has been tilted by 4.2° away from the ⟨110⟩ zone axis [Fig. 3(c)]. The corresponding diffractograms shown together with the image contrasts enable monitoring of the fringe spacings in dependence on orientation deviations. The result of this evaluation proves that the image contrast worsens with increasing angle of lattice tilt, but no systematic deviation of the spacings can be concluded. The image of the untilted particle clearly exhibits two sets of {111} type lattice plane fringes, one of {200} and one of {220}. Upon tilting more than about 10° out of the zone axis, nearly all fringe contrast is lost and mostly weak fringes of only one set of lattice planes remain.

This behavior is completely changed with particles containing planar defects like twin boundaries. The atomic models of an untwinned and a single twinned particle of truncated octahedron shape shown in Fig. 4 may explain how the twinned is derived from the untwinned one by reflecting its upper half at a horizontal atomic plane in the center. This mirror plane, marked by arrows in the twinned one, is called the twin plane or twin boundary because it separates two regions of the particle having different lattice orientation. In ⟨110⟩ zone axis orientation as used to represent the models in Fig. 4, the twin plane is seen end-on, and the two twin segments situated side-by-side exhibit the same, but nearly 72° azimuthally rotated, orientation. An example for this configuration is the particle shown in Fig. 5(a), where white arrows mark the twin plane. In the corresponding

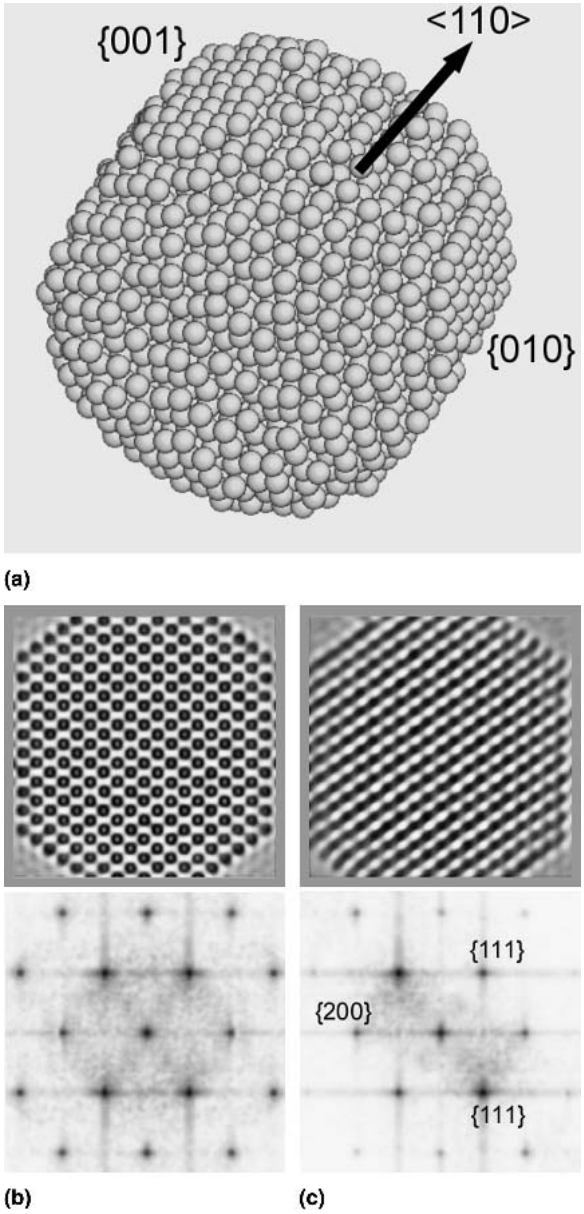

FIG. 3. (a) Atomic model of a nearly 3000 atoms silver nanoparticle in perspective view and (b) image contrast calculations according to this model without and (c) with deviation by 4.2° tilting from the ⟨110⟩ zone axis orientation. The microscope parameters applied are specified in the text.

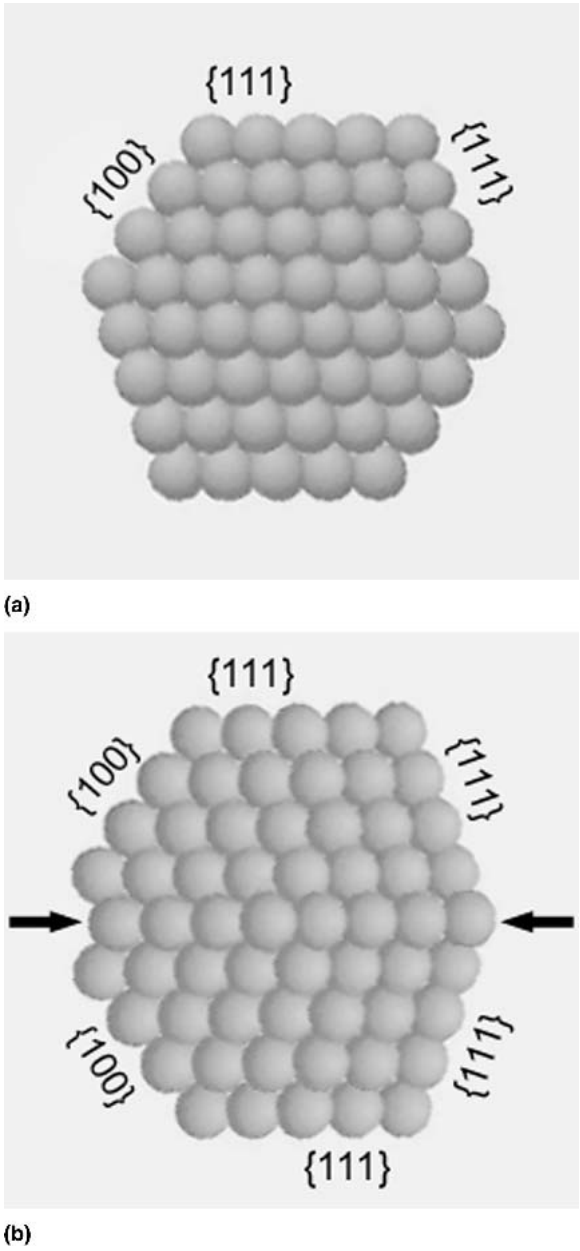

FIG. 4. (a) Atomic model of a truncated octahedron particle without twin fault and (b) in single-twinned configuration where the arrows mark the trace of the twin plane seen end-on.

diffractogram shown in Fig. 5(b), black arrows mark the direction of the twin plane, being identical to one set of {111} lattice planes common to both twin segments. The diffractogram displays the reflections of both lattices connected by streaks along ⟨111⟩ since the reciprocal lattice points are elongated when a crystal contains twins or stacking faults.[25,26]

Upon tilting such a particle, with the twin plane seen end-on, away from the ⟨110⟩ zone axis orientation, the fringe contrast of lattice planes does not worsen as much as it does in single-crystalline particles. With increasing tilting angle, the twin boundary will become invisible, but mostly image contrast of two sets of lattice plane fringes can be seen even if the particle is tilted by about 30°.[26] The reasons for this behavior are (i) the deviation from the initial orientation is different for both twin segments, and (ii) the electron beam consecutively passes through the superimposed twin segments leading to double diffraction effects for some specific orientations. Double diffraction in twinned particles can lead to anomalous images containing atomic column-like contrasts that exhibit nearly 6-fold symmetry as clearly

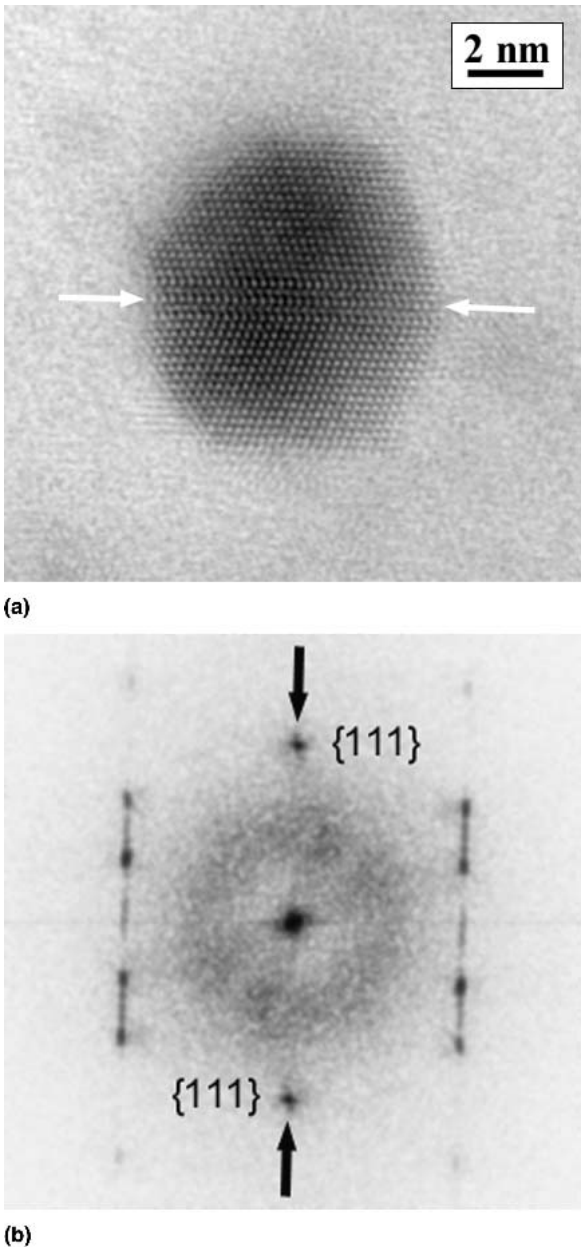

FIG. 5. (a) HREM image of a silver nanoparticle of single twinned truncated octahedron shape in ⟨110⟩ zone axis orientation and (b) corresponding diffractogram, where arrows mark the direction of the twin plane.

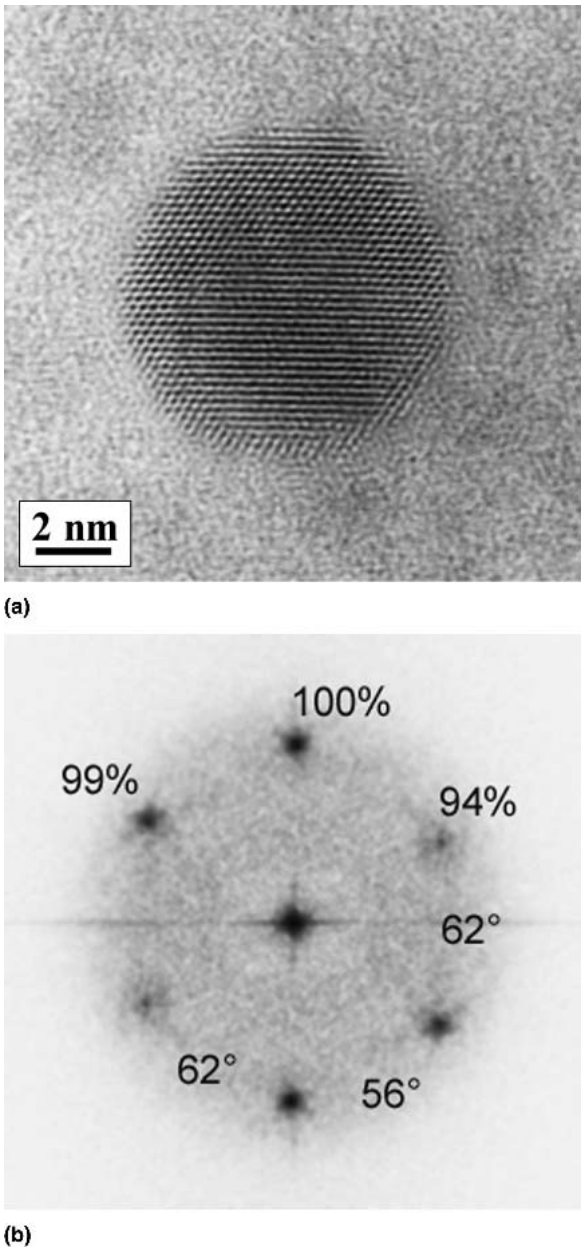

FIG. 6. (a) HREM image of a silver nanoparticle of single twinned cuboctahedron shape and (b) corresponding diffractogram, where three sets of {111}-type reflections occur, with indication of spacings and angular relations. The twin boundary is not visible in the image since it is inclined to the electron beam with one twin unit in nearly ⟨123⟩ and the other in nearly ⟨321⟩ zone axis orientation.

reflected by the corresponding diffractograms.[19,20,26] The anomalous spacings and angular relations of lattice plane fringes are sometimes interpreted in terms of an hcp structure present in such particles instead of the usual fcc lattice.[19] A typical example of such an image is shown in Fig. 6, where the relative distance of diffractogram spot pairs [100% means the {111} spot distance], and their angular relations are indicated. The angle of 56° between the two strong pairs of {111}-type reflections points to double diffraction because of an inclined twin plane as it has been reported repeatedly[20,25,26] where the adjacent twin segments are situated in ⟨123⟩ and ⟨321⟩ orientation with respect to the electron beam. For comparison, Fig. 7 shows the schematic drawing of a cuboctahedron [Fig. 7(a)] as model of a single crystalline particle in ⟨110⟩ orientation like the one in Fig. 2(a), and that of a twinned cuboctahedron [Fig. 7(b)] as model of the particle shown in Fig. 6(a), from which the difference in morphology and electron beam path, marked by dash line arrows, may become clear. It should be noted here that depending on the inclination of the electron beam with

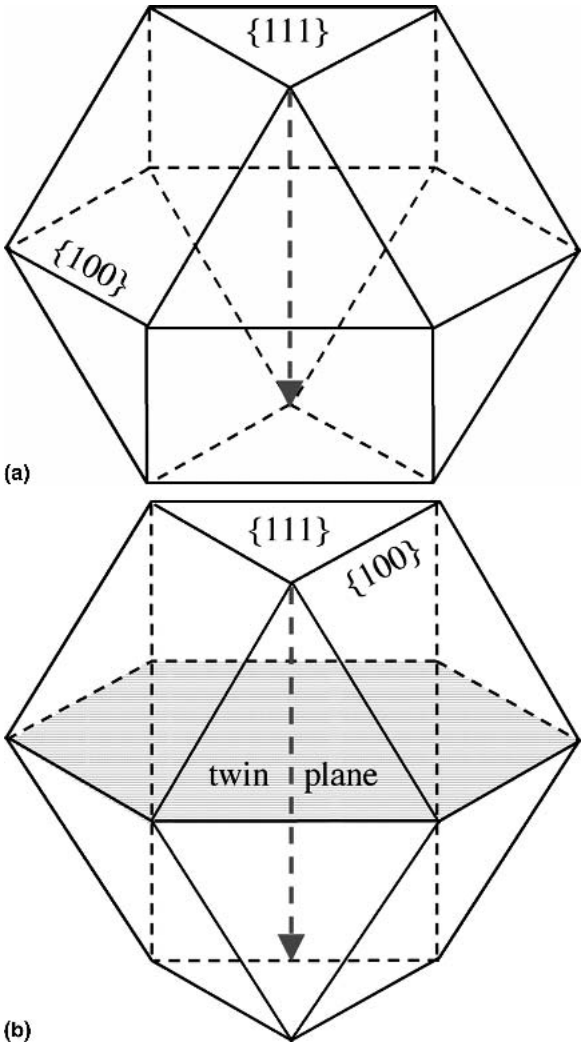

FIG. 7. (a) Schematic drawing of a cuboctahedron with indication of triangular {111} and squared {100} faces, where the dash line arrow marks the ⟨110⟩ direction of the electron beam, and (b) of a single-twinned cuboctahedron, where the dash line arrow marks the electron beam obliquely passing through the twin plane.

respect to the twin plane, the angular relations and spacings of the lattice plane fringes might continuously vary.[26] This effect may introduce an appreciable source of error in any evaluation of lattice contraction or dilatation from spacings of lattice plane fringes unless such measurements are not excluded.

C. Lamellar and cyclic multiply twinned nanoparticles

Twin formation has a considerable effect on the shape and internal structure of nanoparticles, especially in the case of repeated twinning of which two types are known: lamellar and cyclic. Lamellar twins form by repeated twinning on parallel twin planes one after another. Cyclic twins require twinning on nonparallel coplanar twin planes. In fcc metals, low energy twin planes are of {111} type that enclose an angle of 70.53°, being close to $2\pi/5$. Therefore, in these materials 5-fold twinning may form a nearly complete circle giving rise to a whole class of structures based on cyclic twinned segments of mostly tetrahedral or cuboctahedral shape.[15] Identification of the structure of such multiply faulted nanoparticles requires special high symmetry orientations with respect to the electron beam. Figure 8(a) shows an example of a silver nanoparticle in ⟨110⟩ zone axis orientation with several parallel twin lamellae in its center. Because of the nearly spherical shape of the particle its twinned structure can

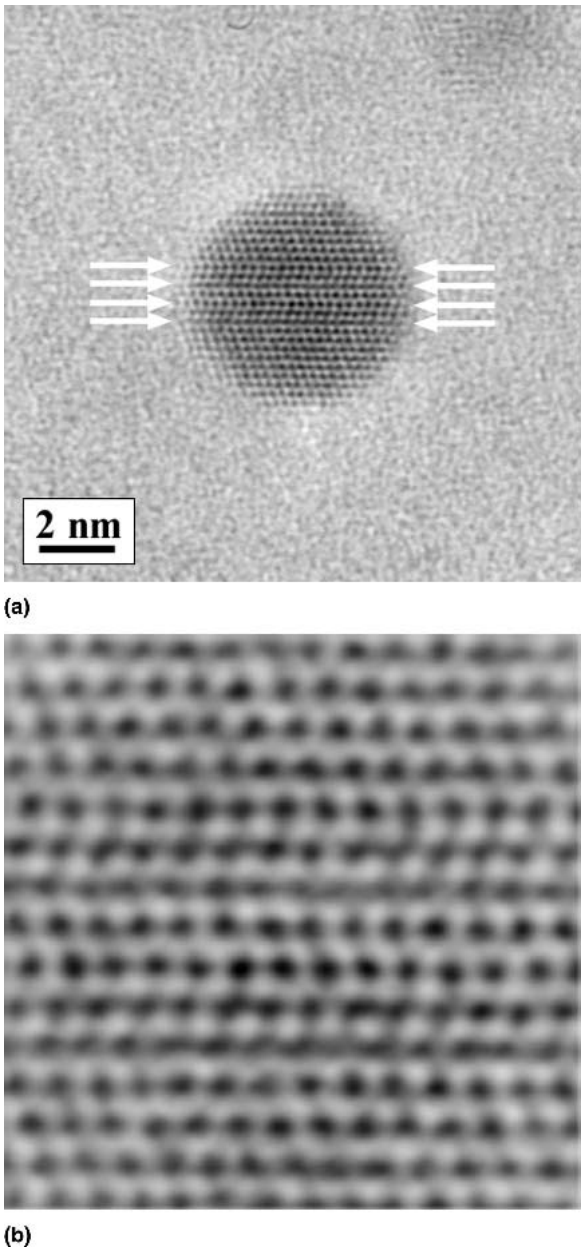

FIG. 8. (a) HREM image of a nearly spherical silver nanoparticle in ⟨110⟩ zone axis orientation with several parallel twin lamellae marked by arrows and (b) a closer view on the twin configuration in a central selection.

be easily overlooked. However, from the selection shown in Fig. 8(b) at higher magnification the closely spaced configuration of twin lamellae and the zigzag-like lattice shift may be recognized. A slightly elongated particle shape results for the silver nanoparticle shown in Fig. 9(a), where the lamellar multiply twinned region marked by arrows is situated outside the particle center. Here again, the higher magnification shown in Fig. 9(b) illustrates the misstacking in the faulted region.

An example of the second type, the cyclic multiply twinned nanoparticles, is shown in Fig. 10, together

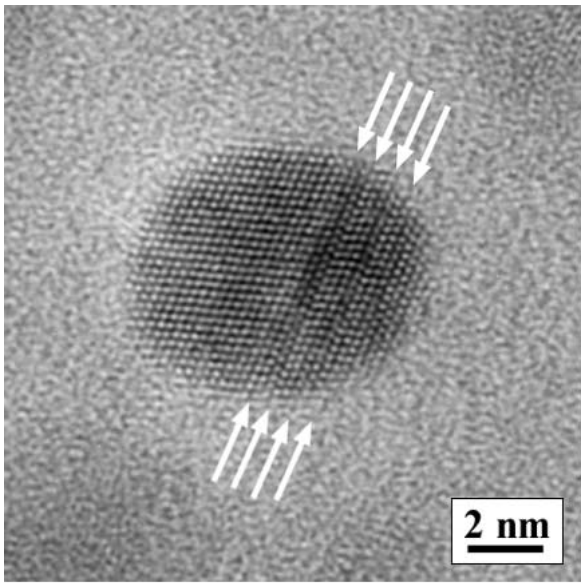

(a)

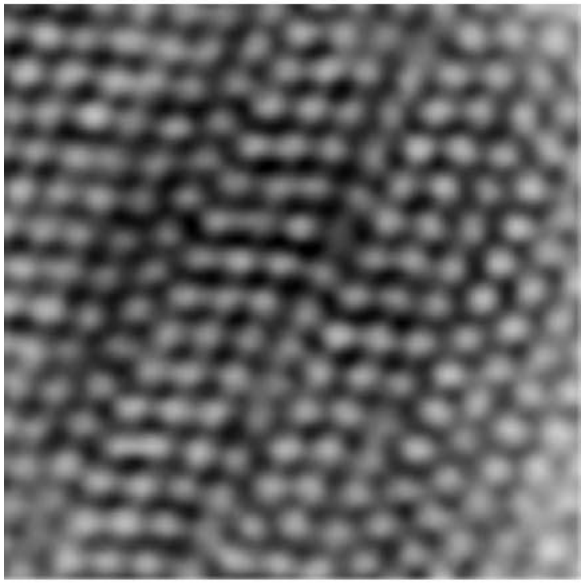

(b)

FIG. 9. (a) HREM image of a slightly elongated silver nanoparticle in ⟨110⟩ zone axis orientation with several parallel twin lamellae marked by arrows and (b) a closer view on the twin configuration in a peripheral selection.

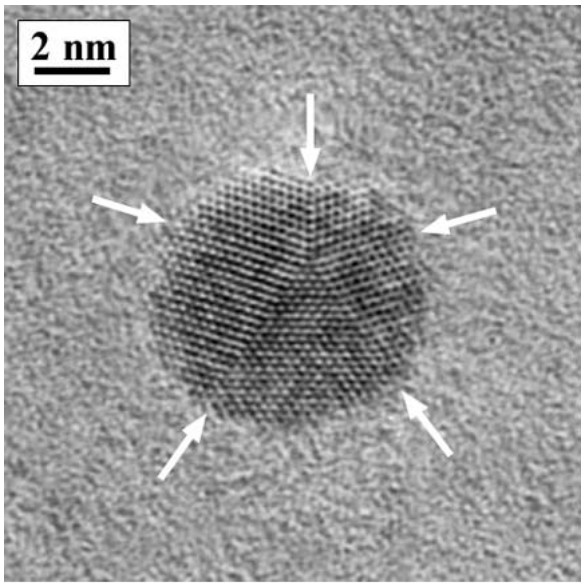

(a)

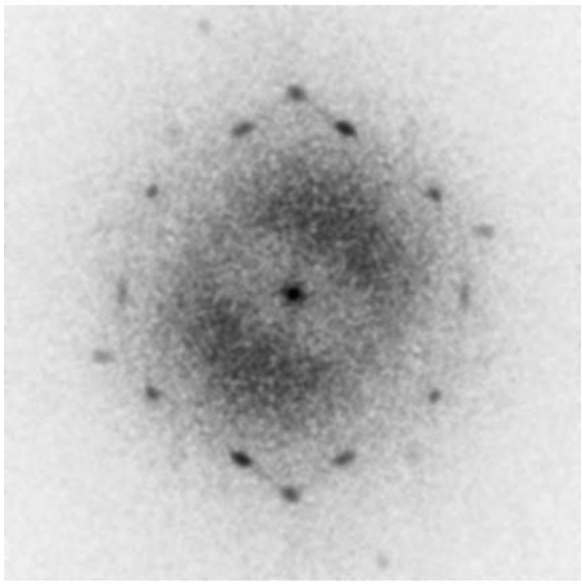

(b)

FIG. 10. (a) HREM image of a multiply cyclic twinned silver nanoparticle with the 5-fold twin junction being parallel to the electron beam and (b) corresponding diffractogram, where {111} and some {200} spots of the twin segments in ⟨110⟩ orientation occur.

with the corresponding diffractogram. Each of the five twin segments situated in ⟨110⟩ zone axis orientation always shares two coplanar {111} faces, the twin planes, with adjacent segments as schematically drawn in Fig. 11(a). The common inner edge of all segments of this decahedron, the 5-fold twin junction, is oriented parallel to the electron beam enabling a clear representation of the internal structure as well as some deviations from the model shape. In Fig. 10(a), the arrows point to the twin boundaries that exhibit slight grooving where they

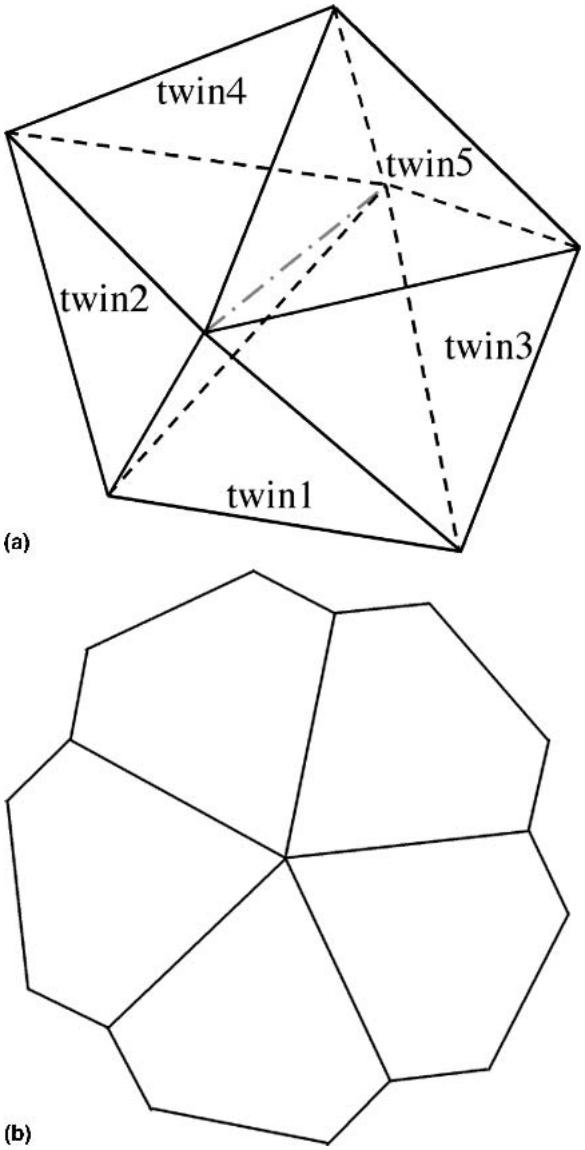

FIG. 11. Schematic drawing of a decahedron composed of five segments of tetrahedron shape situated in twin position to each other and arranged around a common 5-fold axis (a) in perspective view and (b) with the twin planes and 5-fold axis seen end-on, where a certain twin boundary grooving is considered.

emerge to the particle surface. The extent of this frequently observed surface modification schematically represented in Fig. 11(b) depends on the respective growth conditions.[15] Evaluation of the spacings and angular relations of the {111} and {200} type lattice plane fringes by means of the diffractogram in Fig. 10(b) revealed no deviation from the fcc lattice of the twin segments. Therefore, a lattice transformation to tetragonal or orthorhombic structures can be excluded even if no additional lattice defects have been found, similar to the 5-fold twinned silver nanorods deposited on a substrate.[27]

Besides the 5-fold orientation of decahedral particles with their 5-fold axis parallel to the electron beam, another high symmetry orientation is the one where the 5-fold axis is situated perpendicular to the electron beam, while simultaneously one twin plane is coplanar with the beam. Because of the superposition of twin segments in different orientation double diffraction results in complicated patterns of lattice plane fringes and Moiré fringes.[27] Anomalous contrast features arise upon tilting the 5-fold axis by about 13° away from the direction perpendicular to the electron beam.[20,28] Such an image

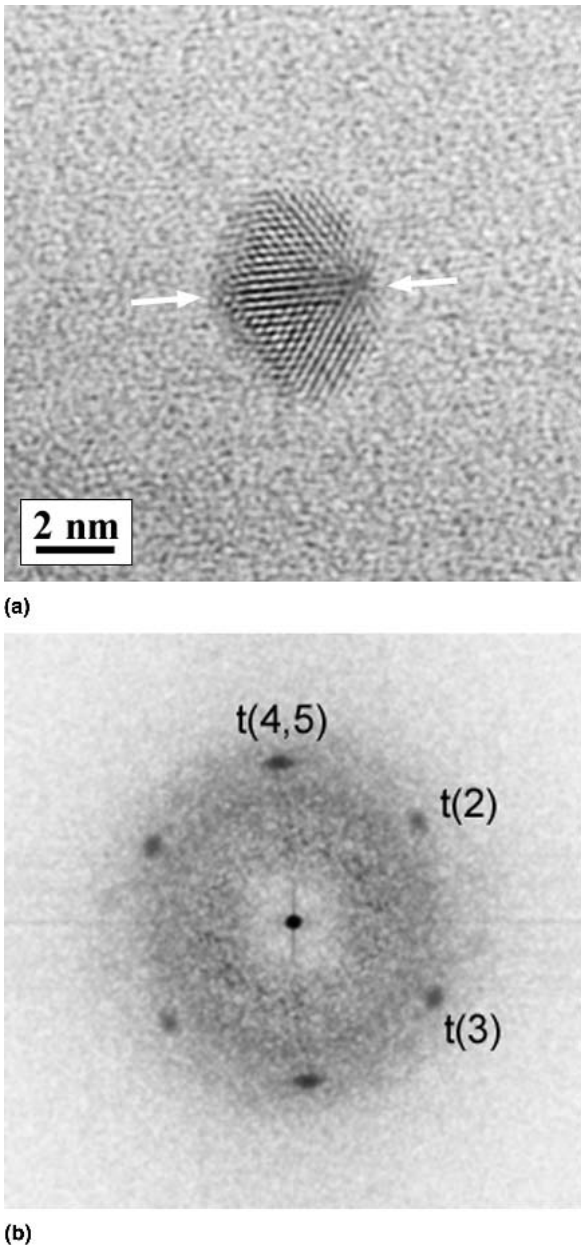

FIG. 12. (a) HREM image of a silver nanoparticle of truncated decahedron shape, where the 5-fold axis (marked by arrows) is inclined to the electron beam, and (b) corresponding diffractogram with three sets of {111}-type spots due to different twin segments as marked in Fig. 13(b).

accompanied by the corresponding diffractogram is shown in Fig. 12. In both, the real space and the reciprocal space image, three sets of {111} type fringes can be recognized. One of them, running throughout the whole particle image parallel to the arrows that mark the 5-fold axis, is due to lattice planes parallel to the twin plane between twin segments 4 and 5 as schematically shown in Fig. 13. In Fig. 13(a), an accordingly tilted decahedron with certain truncation of the peripheral edges[20,29] to match the particle image in Fig. 12(a) is drawn in side view to illustrate the inclination of its 5-fold axis with respect to the electron beam. Figure 13(b) shows a schematic top view of such a particle with indication of the uppermost twin segments 4 and 5, and the twin segments 2 and 3 located underneath, as well as the bottom twin segment 1. Twin segments 2 and 3 are situated such that always one set of {111} fringes parallel to one of their external faces appear in the upper and the lower half of the image in Fig. 12(a), respectively. This situation is also marked in the diffractogram in Fig. 12(b). The unique pattern of three sets of {111} type spots where two of them (t2 and t3) are rotated by 56° each with respect to the third one (t4, t5) may help to identify such unclearly arranged particles.

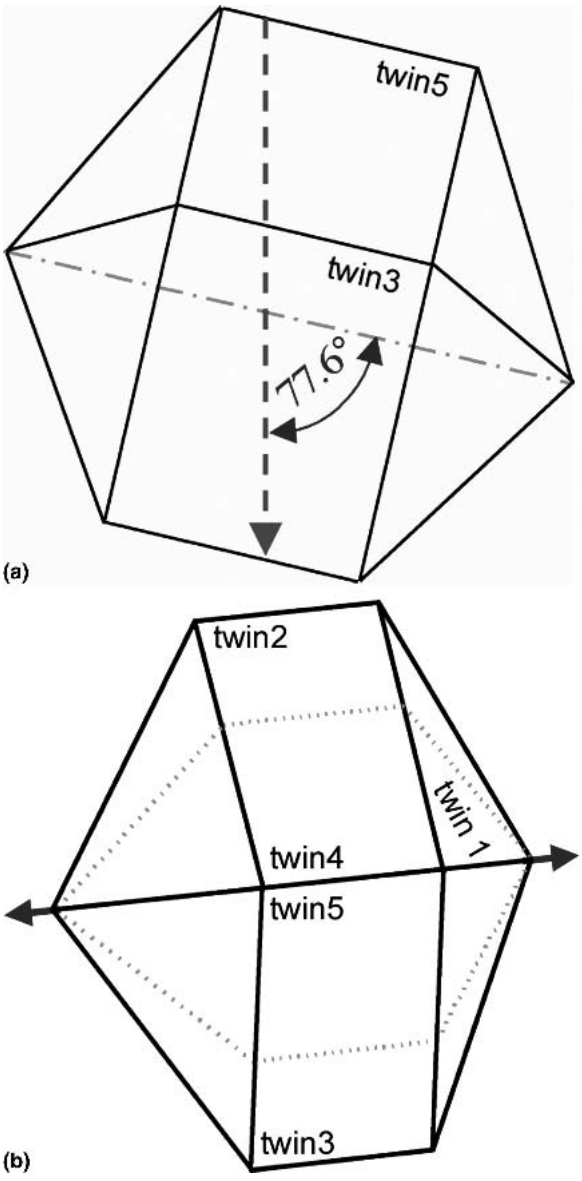

FIG. 13. Schematic drawing of a truncated decahedron (a) in side view with the 5-fold axis (dash dot line) inclined by ~78° to the electron beam (dash line arrow) and (b) in top view with a twin plane between two twin segments (4) and (5) parallel to the electron beam.

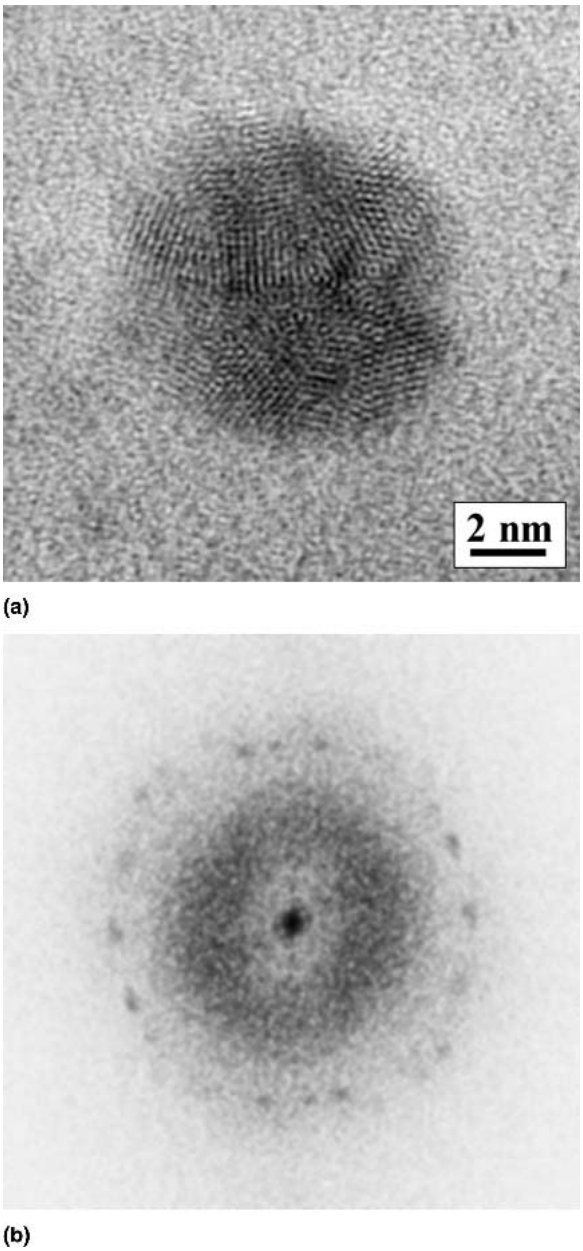

FIG. 14. (a) HREM images of silver nanoparticles of icosahedron shape situated in low symmetry orientation with irregular patterns of superimposed lattice plane fringes and (b) corresponding diffractogram.

To proceed one step further with the complicated configuration and unclear arrangement of silver nanoparticles embedded in glass, we finally turn to cyclic multiple twinned particles of icosahedron shape. They are composed of 20 equally sized twin segments of tetrahedron shape that share six 5-fold axes and one common point at the center.[15] Each of the involved tetrahedra exhibits only one triangular external face of {111} type so as to minimize the surface energy by approaching a spherical shape. On crystalline substrates, these rather complicated structures are frequently found in a number of high-symmetry orientations that allow identification from HREM images by means of characteristic patterns in real and in reciprocal space that may be considered as fingerprints.[14–16,20] For nanoparticles of icosahedron shape embedded in a glass matrix, there are no common orientation relations and high-symmetry orientations may only occasionally occur. A typical example of those we have found in our silver-doped glasses is shown in Fig. 14 together with the corresponding diffractogram. At first sight no regular patterns may be recognized and no assignment to known arrangements like the one shown as a schematic drawing in Fig. 15(a) is possible. To find an adequate low-symmetry orientation like the example shown as a schematic drawing in Fig. 15(b), extensive image contrast calculations considering through-focus series and various kinds of tilting sequences[29] are required. Such rather confused contrast patterns may also be due to modification of the icosahedra during growth by attachment of additional twin segments as considered in molecular dynamics calculations[30] that may lead to imperfect intermediate or compound structures like the extended icosahedron observed upon confined growth.[31] However, from the schematic drawings in Fig. 15, it is quite clear that the HREM image contrast features for both types of orientation result from double diffraction effects due to superposition of two or even more twin segments. Therefore, it is of no use to consider measurements of spacings of lattice plane fringes and angular relations obtained from such images for systematic evaluation of the state of stress of silver nanoparticles in glass.

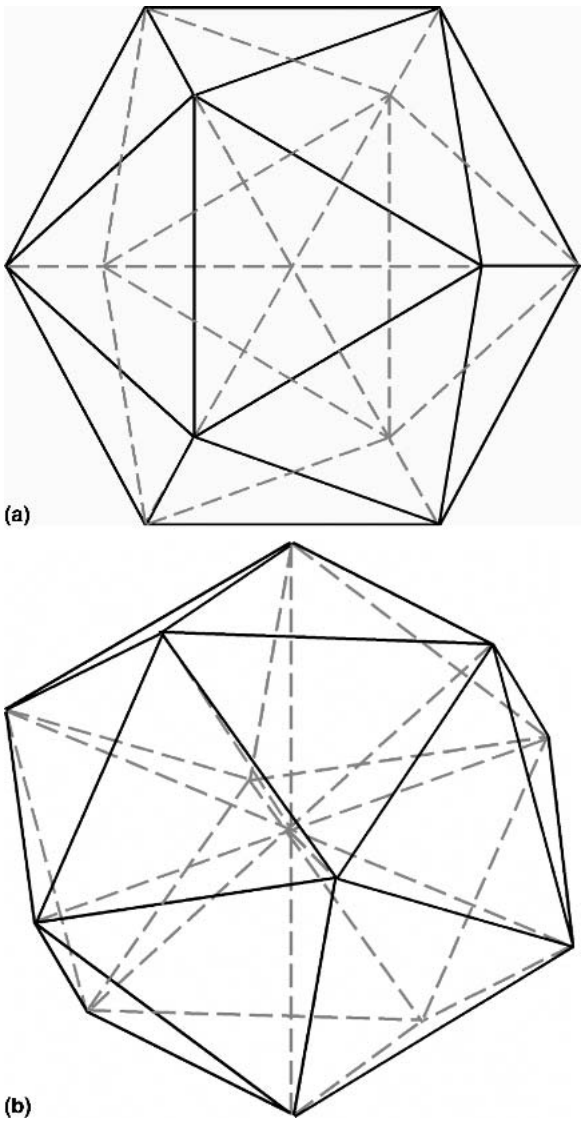

FIG. 15. Schematic drawing of an icosahedron composed of 20 segments of tetrahedron shape situated in twin position to each other and arranged around 6 common 5-fold axes in (a) a high symmetry orientation and (b) a low symmetry orientation.

IV. CONCLUSIONS

Silver nanoparticles embedded in soda-lime silicate glass exhibit a variety of forms comparable to those of non-embedded transition metal particles. Although we have found a certain preference for some of them varying for different routes of synthesis and processing, there is no principal difference in the particle forms. These are single-crystalline, single-twinned, and multiple twinned particles based on truncated octahedron or cuboctahedron shape that exhibit the fcc lattice of bulk silver. The multiple twinned particles may occur with parallel twin lamellae or with cyclic twinned segments. Cyclic twinning around 5-fold axes results in specific particle morphologies based on the decahedron or the icosahedron shape. For the particles of icosahedron shape, rather seldom observed in glass, no clear lattice characteristic can be given until now.

Evaluation of the state of stress as well as of lattice distortions in silver nanoparticles embedded in glass by HREM imaging of lattice plane fringes requires consideration of lattice spacings and angular relations at single-crystalline species only or where double diffraction due to superposition of twin segments can be excluded. The structural features essential for the reliability of such measurements in the presence of twin boundaries are configurations that may not lead to serious confusion

because of anomalous image contrast features. This can be assumed for single-twinned particles of cuboctahedron shape and 5-fold twinned particles of decahedron shape if the twin planes are imaged end-on to result in the same ⟨110⟩ zone axis orientation of all twin units.

ACKNOWLEDGMENT

This work was supported by the German Research Foundation (DFG) in the frame of a Collaborative Research Centre (SFB 418).

REFERENCES

1. C. Mohr, H. Hofmeister, and P. Claus: The influence of the real structure of gold catalysts in the partial hydrogenation of acrolein. *J. Catal.* **213,** 86 (2003).
2. W.P. Cai, H. Hofmeister, and M. Dubiel: Importance of lattice contraction in surface plasmon resonance shift for free and embedded silver particles. *Eur. Phys. J. D* **13,** 245 (2001).
3. K.J. Berg, A. Berger, and H. Hofmeister: Small silver particles in glass surface layers produced by sodium-silver ion exchange—Their concentration and size depth profile. *Z. Phys. D* **20,** 309 (1991).
4. A. Berger, K.J. Berg, and H. Hofmeister: Aggregates of small silver particles in surface layers of glasses – electron microscopy and optical microspectroscopy. *Z. Phys. D* **20,** 313 (1991).
5. P.W. Wang: Formation of silver colloids in silver ion-exchanged soda-lime glasses during annealing. *Appl. Surf. Sci.* **120,** 291 (1997).
6. A. Meldrum, R.F. Haglund, Jr., L.A. Boatner, and C.W. White: Nanocomposite materials formed by ion implantation. *Adv. Mater.* **13,** 1431 (2001).
7. H. Hofmeister, M. Dubiel, H. Goj, and S. Thiel: Microstructural investigation of colloidal silver embedded in glass. *J. Microsc.* **177,** 331 (1995).
8. M. Dubiel, H. Hofmeister, E. Schurig, E. Wendler, and W. Wesch: On the stress state of silver nanoparticles in ion-implanted silicate glasses. *Nuclear Instr. Meth. Phys. Res. B* **166-167,** 871 (2000).
9. M. Dubiel, H. Hofmeister, and E. Schurig: Interface effects at nanosized silver particles in glass. *Rec. Res. Devel. In Appl. Phys.* **1,** 69 (1998).
10. M. Klimenkov, S. Nepijko, H. Kuhlenbeck, M. Bäumer, R. Schlögl, and H-J. Freund: The structure of Pt-aggregates on a supported thin aluminum oxide film in comparison with unsupported alumina: A transmission-electron-microscopy study. *Surf. Sci.* **391,** 27 (1997).
11. L.D. Marks: Experimental studies of small particle structures. *Rep. Prog. Phys.* **57,** 603 (1994).
12. S. Iijima: Electron microscopy of small particles. *J. Electron Microsc.* **34,** 249 (1985).
13. S. Iijima and T. Ichihashi: Stacking disorder and twin deformation in small metal clusters. *Mater. Trans., JIM.* **31,** 582 (1990).
14. J.M. Montejano-Carrizales, J.L. Rodríguez-Lopéz, C. Guiterrez-Wing, M. Miki-Yoshida, and M. José-Yacaman: Crystallography and shape of nanoparticles and clusters, in *Encyclopedia of Nanoscience and Nanotechnology*, Vol. 2, edited by H.S. Nalwa (American Scientific, Stevenson Ranch, CA, 2004), p. 237.
15. H. Hofmeister: Fivefold twinned nanoparticles, in *Encyclopedia of Nanoscience and Nanotechnology*, Vol. 3, edited by H.S. Nalwa (American Scientific, Stevenson Ranch, CA, 2004), p. 431.
16. J. Urban: Structure of nanoclusters by high-resolution electron microscopy, in *Encyclopedia of Nanoscience and Nanotechnology*, Vol. 10, edited by H.S. Nalwa (American Scientific, Stevenson Ranch, CA, 2004), p. 161.
17. C.Y. Yang: Crystallography of decahedral and icosahedral particles I. Geometry of twinning. *J. Cryst. Growth* **47,** 274 (1979).
18. Y. Wu, Q. Chen, M. Takeguchi, and K. Furuya: High-resolution transmission-electron-microscopy study on the anomalous structure of lead nanoparticles with UHV-MBE-TEM system. *Surf. Sci.* **462,** 203 (2000).
19. M. José-Yacaman, R. Herrera, A. Gómez, S. Tehuacanero, and P. Schabes-Retchkiman: Decagonal and hexagonal structures in small gold particles. *Surf. Sci.* **237,** 248 (1990).
20. P-A. Buffat, M. Flüeli, R. Spycher, P. Stadelmann, and J-P. Borel: Crystallographic structure of small gold particles studied by high-resolution electron microscopy. *Faraday Discuss.* **92,** 173 (1991).
21. M. Dubiel, S. Brunsch, W. Seifert, H. Hofmeister, and G.L. Tan: Stress state of silver nanoparticles embedded in a silicate glass matrix investigated by HREM and EXAFS spectroscopy. *Eur. Phys. J. D* **16,** 229 (2001).
22. M. Dubiel, H. Hofmeister, G.L. Tan, K-D. Schicke, and E. Wendler: Silver diffusion and precipitation in glass by ion implantation. *Eur. Phys. J. D* **24,** 361 (2003).
23. W. Rasband: NIH Image public domain software, U.S. National Institute of Health, Bethesda, MD (http://rsb.info.nih.gov/nih-image/).
24. P. Claus and H. Hofmeister: Electron microscopy and catalytic study of silver catalysts: Structure sensitivity of the hydrogenation of crotonaldehyde. *J. Phys. Chem. B* **103,** 2766 (1999).
25. D.W. Pashley and M.J. Stowell: Electron microscopy and diffraction of twinned structures in evaporated films of gold. *Philos. Mag.* **8,** 1605 (1963).
26. H. Kohno, N. Ozaki, H. Yoshida, K. Tanaka, and S. Takeda: Misleading fringes in TEM images and diffraction patterns of Si nanocrystallites. *Cryst. Res. Technol.* **38,** 1082 (2003).
27. H. Hofmeister, S.A. Nepijko, D.N. Ievlev, W. Schulze, and G. Ertl: Composition and lattice structure of fivefold twinned nanorods of silver. *J. Cryst. Growth* **234,** 773 (2002).
28. A. Renou and J.M. Penisson: Direct atomic imaging in small multiply twinned palladium particles. *J. Cryst. Growth* **78,** 357 (1986).
29. K. Koga and K. Sugawara: Population statistics of gold nanoparticle morphologies: Direct determination by HREM observations. *Surf. Sci.* **529,** 23 (2003).
30. F. Baletto, C. Mottet, and R. Fernando: Microscopic mechanism of the growth of metastable silver icosahedra. *Phys. Rev. B* **63,** 155408 (2001).
31. S.A. Nepijko, H. Hofmeister, H. Sack-Kongehl, and R. Schlögl: Multiply twinned particles beyond the icosahedron. *J. Cryst. Growth* **213,** 129 (2000).